Determination of Heat Capacities using Modern Calorimetry Techniques

Daniel Elston
School of Physics - BSc Year 2
University of Bristol

March 12, 2022

Abstract

Implementing modern calorimetry techniques with the use of cryogenic liquids, a change in mass of a nitrogen calorimeter system can be used to obtain the latent heat of vaporisation of nitrogen and the heat capacity of various samples. Understanding the heat capacity of a substance is of great use in the renewable energy industry, governing how much thermal energy can be efficiently stored at one time. A value for the latent heat of vaporisation of nitrogen was found to be 213.8±3.8 kJ/kg, compared to theoretical values 200.0 kJ/kg. A possible cause for such a large difference includes heat conduction into the system through the equipment used. Heat capacity at constant volume of samples aluminium, rock salt, carbon, zinc, copper and lead were found at initial temperatures of 293K and 194K. Results for heat capacities were all within margin of error. Although accurate, results were unreliable and possible improvements have been suggested. The results conclude that a greater number of atoms per gram of mass corresponds to a greater heat capacity, agreeing with the degrees of freedom theory.

Contents

1 Introduction

Heat capacity of different substances has been well documented over the last two centuries. As technology advances, a much wider range of temperatures are now within reach and errors given for heat capacities have minimised [1]. Simple experiments devised such as calorimetry, which in the past would be prone to vast amounts of error, can be performed with modern technology allowing for minimal error and a high degree of accuracy.

The most basic calorimeter, made in 1845, would make use of an enclosed vessel of water, in which a thermometer was fitted. This vessel would be heated, then plunged into a solution and used as a stirrer. The temperature of the solution was then measured at frequent intervals until it became constant [2].

A modern comparison consists of digital measuring devices coupled with updated equipment and a cryogenic substance, in this case, nitrogen. The sample at a given temperature will be submerged into the nitrogen and the change in mass of the system will be recorded. Liquid nitrogen has a boiling point of 77K. The phase changing qualities at such low temperatures make cryogenic substances well suited for high precision calorimetry and the determination of a samples heat capacity. Human error can be avoided by keeping more variables constant, such as not stirring the system and producing kinetic energy.

Determining heat capacity and how a substance's heat capacity can be altered is of great technological use, particularly in solar thermal-energy storage. Research grows ever more important as the race for clean, renewable energy continues. Typical solar thermal-energy storage facilities require the storage medium to have high heat capacity and thermal conductivity [3]. This enables such facilities to store more heat and radiate less reducing demand for fossil fuels.

Furthermore, research suggests that heat capacity can give a lot of information relating to a substances superconducting qualities. There seems to be a link between resistivity and heat capacity at low temperatures [4]. Advancements in superconductors will lead to a more efficient use of electricity and power grid.

2 Theory

Energy is supplied to the calorimetry system in the form of heat. The latent heat of vaporisation is defined as the heat required to change one gram of liquid at its boiling point, to gas, under standard atmospheric pressure [5] given by,

$$L_v = Q/\Delta m_1 \tag{1}$$

where Q is heat and Δm$_1$ is the change in mass of the nitrogen. An equation for heat as a function of temperature,

$$Q = m \int_{T_i}^{T_f} c(T)dT \tag{2}$$

where m is mass of sample, c is specific heat capacity of sample, T is temperature.

The heat capacity of a substance is defined as the amount of heat required to raise the temperature of that substance by one degree [6]. The specific heat of a substance is the amount of heat required to raise the temperature by one degree per unit mass, derived using equation 2 and equation 1,

$$c = \Delta m_1 L_v / m_2 \Delta T \tag{3}$$

where m$_2$ is the mass of a sample and ΔT is the change in temperature.

2.1 Degrees of Freedom

Classical theories of specific heat are accurate at high temperatures due to their understanding of degrees of freedom. There exist three classifications of degrees of freedoms. The translational degree of freedom, allowing for movement on the x, y and z axis. Rotational, allowing for the molecule to spin on its axis. Finally, vibrational which involves contraction and expansion of the bonds between atoms in a molecule. The atoms contract and expand toward one and other about their equilibrium position. The more degrees of freedom a molecule has, the more ways it can store energy. The translational degree of freedom in the form of kinetic energy is seen in single atoms or diatomic molecules. The rotational and vibrational degrees of freedom limited to polyatomic molecules have stored energy in the form of elastic potential. As heat is supplied to a system, more degrees of freedom are 'unfrozen' and thus able to store more energy. For example, a diatomic molecule with 2 degrees of freedom has kinetic energy stored as it moves on the x, y and z axis, but also elastic potential as it spins about its equilibrium. The more atoms per gram of a substance, the more degrees of freedom a substance has, the higher its capacity to store heat.

2.2 Early Theories

The Dulong and Petit model of specific heat capacity employs a classical mechanics approach, suggesting that substances atoms have three degrees of freedom and each atom has vibrational energies. Specific heat can be calculated using the theory of degrees of freedom,

$$C = 3k_B N \tag{4}$$

where N is number of atoms, k$_\mathrm{B}$ is the Boltzmann's constant and the constant 3 is the degrees of freedom of an atom. This leads to a temperature independent specific heat [7]. Due to the theory of degrees of freedom,

equation (4) yielded acceptable results of heat capacity provided that an intermediate to high temperature is used. It was clear at the time that this theory was flawed due to deviation of the heat capacity of diamond at room temperature as well as other solids at low temperatures [8].

The Einstein model proposed that atoms in a solid were arranged in a lattice form and acted as harmonic oscillators, each undergoing individual and independent harmonic vibrations about their equilibrium lattice position. Einstein further proposed that energy of oscillators must be quantized and that each atom vibrates with the same frequency [8].

While accurate results were observed using this model from high to very low temperatures, Einstein's idea of the harmonic oscillations of atoms occurring individually was wrong. If this were the case, a random walk of heat diffusion would be observed. Furthermore, oscillations are a result of waves propagating through the lattice.

2.3 Debye Theory

The Debye theory simplified the problem being faced within the study of heat capacity of solids. Its basic assumptions are to consider solids as continuous, homogeneous, elastic mediums able to support the propagation of longitudinal waves [9]. Speed of wave propagation would therefore be equal to the speed of sound in accordance with the classical elastic continuum. This assumes velocity of sound waves in a solid are constant for all frequencies. The ability to propagate waves infers that the atoms are no longer isolated and are instead, free to oscillate together throughout the medium, disagreeing with Einstein's theory.

The Debye theory agrees well with results at low to high temperatures for single atom per unit cell solids, however fails for crystalline solids with more complex lattice structures [8]. Furthermore at very low temperatures, the Debye approximation must be made. In summary, the Debye model treats solids as elastic lattices of atoms moving together, capable of transmitting vibrational energy as longitudinal waves, known as phonons, at the speed of sound. The model is not perfect and more research is needed.

2.3.1 Phonons

The energy of a lattice vibration is quantized, called a phonon in analogy with photon of electromagnetic waves [10]. The quantized energy of a phonon is given by $E = \hbar\omega$, where ω is angular frequency given by $\omega = \nu_s|\vec{q}|$, where ν_s is the speed of sound waves and $|\vec{q}|$ is the wave vector.

Phonons are classified into lower and higher vibrational energies. Acoustic phonons correspond to low vibrational energy modes of a solid and act as a collective motion of atoms. Optical phonons correspond to high vibrational energy modes and act more individually throughout the medium [8].

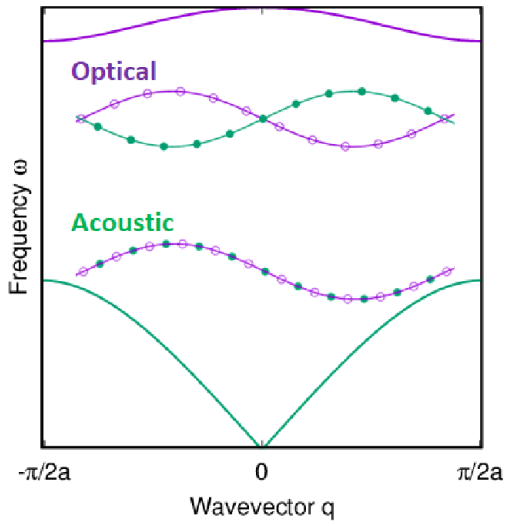

Figure 1: Difference between optical phonons (top) and acoustic phonons (bottom). Individual phonon wavelength and frequencies can be observed [11].

The difference in energy generally comes from the displacement of an atom, the higher the displacement of an atom from its equilibrium position, the higher the phonon energy [10]. As shown in figure 1, the optical phonon is susceptible to interference and therefore some of these phonons experience destructive interference, explaining their individuality throughout the medium. The acoustic phonon transmits as more of a singular wave form over a collection of atoms. Furthermore, figure 1 clearly shows the space and therefore displacement between individual atoms is far greater for optical phonons compared to the acoustic phonon, relating to a higher degree of energy.

2.3.2 Debye Frequency & Temperature

Phonons are restricted to certain energy modes, known as their density of state. This is similar to the particle in a box theory for quantum mechanics, only now there is a limit to which energy the particle can reach and the box is now the solid that the phonon is propagating in. The density of state is a description of allowed states (or modes) of phonons, per volume at a given energy [12]. For example, a very compact lattice structure may only allow for the propagation of high frequency phonons. Therefore, phonons have a cut off frequency that they cannot go above which limits available states. This limit is called the cut off frequency or Debye frequency.

Characteristics of a samples material, such as lattice spacing or structure, will generally define the cut off frequency. Regardless of the substance, a phonon's

density of state cannot yield a frequency higher than the cut off frequency which corresponds to the smallest distance between atoms in a lattice. An equation for the cut off frequency of phonons in a medium proposed by Debye [10],

$$\omega_D^3 = 6\pi^2 \nu_s^3 N/V \tag{5}$$

where N is number of primitive cells in a sample, which is also equal to the total number of acoustic phonon modes, and V is volume of sample.

The temperature at which the cut off frequency occurs in a given substance is known as the Debye temperature. Equation 5 can be used together with the Boltzmann's constant, to derive an expression for the Debye temperature,

$$\theta_D = \hbar \nu_s \omega_D / K_B \tag{6}$$

. This is the highest frequency mode the phonons in a medium can reach and characterises physical properties of a substance such as thermal conductivity and heat capacity [10]. At this temperature all degrees of freedom are exhausted for a solid lattice. This translates to a plateau for the heat capacity of a solid. Above the θ_D, the Petit and Dulong model holds and the heat capacity of a solid is given by equation 4. For temperatures far below the θ_D however, we introduce a concept called the Debye approximation T^3.

2.3.3 Debye Approximation

At very low temperatures, it is intuitive that phonons of longer wavelength and lower frequency exist more abundantly. Lower frequency corresponds to lower energy and therefore only acoustic phonons are produced. This is not to say that some interference and therefore optical phonons could not occur, but in numbers small enough to disregard [10].

At temperatures less than 15K, the Debye approximation T^3 yields acceptable results. At such low temperatures we only consider acoustic energy modes of phonons and a single degree of freedom contributing to the heat capacity of a sample. The Debye approximation for heat capacities at temperatures far below the Debye temperature,

$$C_v = 234 N K_B (T/\theta_D)^3 \tag{7}$$

agrees well with experimental results. A more in-depth derivation for all equations can be seen in reference [10].

3 Experimental Method

3.1 Latent Heat of Vaporisation of N_2

An independent, reliable result for the latent heat of vaporisation of nitrogen was determined. Using a calorimeter and supplying heat to the system through an electrical circuit shown by figure 2, the change in mass of the system was measured. A value for the natural boil off was measured separately by removing the heating element and measuring the change in mass at regular time intervals. This was subtracted from final change in mass values.

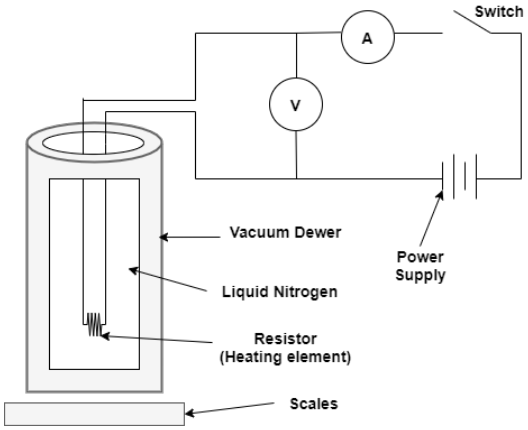

Figure 2: Schematic of apparatus used to measure latent heat of vaporisation of nitrogen.

As the system was heated, a phase transition occurred where liquid nitrogen was vaporised and escaped the dewer. Varying power, the change in mass was recorded on software over time. Using equation 1 and that $Q = E = Pt = VI$, a graph was used to find the latent heat of vaporisation of nitrogen.

3.2 Heat Capacity of Samples

The heating element and circuit from the apparatus show in figure 2 was removed. Samples of constant volume were suspended above the dewer with string and submerged in the nitrogen, as shown in figure 3. Suspension enables the entire surface area of the sample to be submerged, reducing error in results. The mass of each sample was measured and recorded.

The room temperature samples act as the heating element and the change in mass of the system over time was recorded with software. The use of software is important as it eliminates human error when recording data. The samples came in solid cylindrical shapes of varying densities. Rock salt, however, was in the form of many small crystals rolled up in an aluminium foil shell before submersion.

The same method and recording of data, used above, was applied. Samples were first submerged in solid carbon dioxide, known as dry ice. This reduces the initial temperature to 194K, instead of room temperature, highlighting how varying the initial temperature effects final results. To summarise, a temperature change of 216K was observed using nitrogen, then a temperature change of 117K using dry ice.

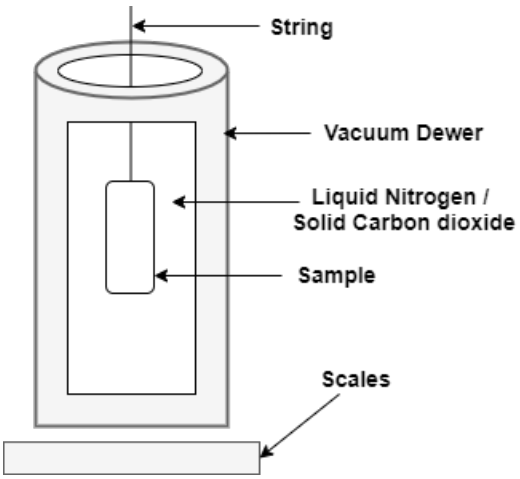

Figure 3: Schematic of apparatus used to measure latent heat of vaporisation of nitrogen.

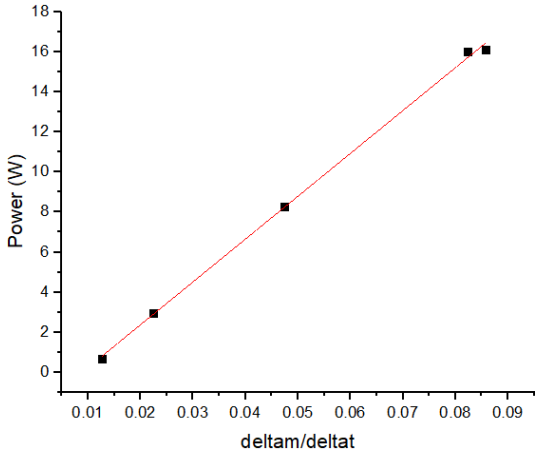

Figure 5: Effect of increasing power on the systems mass.

4 Results

4.1 Latent Heat of Vaporisation of N_2

A natural boil off of 8.9×10^{-6}kg/s was measured from the gradient of figure 4. A value of 213.8±3.8 kJ/kg was determined, in comparison with theoretical value of 200.0 kJ/kg, from a calculated fit of figure 5 after subtracting the boil off gradient.

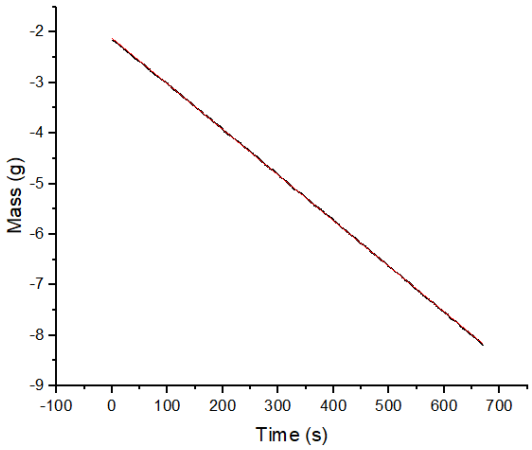

Figure 4: Natural boil off of liquid nitrogen at room temperature.

The results appear linear as seen in figure 5 with slight deviations at greater powers. The χ value of figure 5 is within 1×10^{-6} further highlighting the linearity of results.

Observations at higher powers may improve final value, but could also produce unwanted heat in the form of resistance in the wire or internal energy in the battery that will conduct through the wire. Intuitively the more heat supplied to the system, the more boil off would be observed, agreeing with results.

4.2 Heat Capacity of Samples

Graphs used to determine heat capacity using liquid nitrogen and dry ice are included in the appendix. Due to all graphs from both parts of the experiment sharing common features, figure 6 is given as an aid.

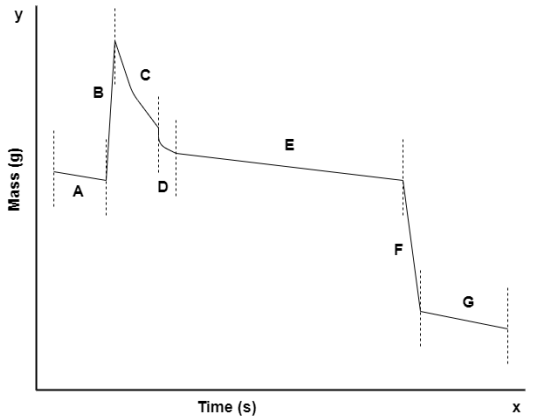

Figure 6: Diagram showing evolution of mass of system. Each feature labelled from A to G.

Measurements were taken of the natural boil off before the sample is added and then after the sample is removed from the system. This is shown by areas A and G shown in figure 6. This allows for extrapolation giving two y-intercept values for an accurate initial and final mass of the system. To account for the natural boil off of nitrogen, the value of 8.9×10^{-6}kg/s calculated previously is subtracted from the final change in mass.

Area B and F corresponds to the sample being added and removed from the system. A buoyancy force was exerted on the scales giving an apparent weight. This change in mass should be disregarded as the weight added to the system from the sample is insignificant to final results. The extrapolation technique discussed above accounts for this sudden change in mass and does not effect final results.

Area C shows a great change in mass in the system. At the peak, the added sample was at room temperature and quickly begins to dissipate stored energy to the surrounding nitrogen, causing a boil off and a large change in mass. This area is the of great importance as it corresponds directly to heat capacity.

An anomalous result was seen in area D, where a relatively large amount of mass was quickly lost, due to the Laden Frost affect. The sample has so much stored heat, compared to the surrounding nitrogen, that the nitrogen was vaporised before touching the sample. This creates a nitrogen gas layer surrounding the sample. As the sample's temperature approaches 77K, the gas bubble was released and a large change in mass was observed. Area E shows the system reaching thermal equilibrium. The change in mass for this area was solely due to natural boil off.

Unfortunately, due to varying sample masses, it was difficult to interpret each graph and draw conclusions by comparison. Table 1 has been included as an aid.

Table 1: Specific heat of samples at different initial temperatures, compared to theoretical values.

Sample	c(T_i=293K) kJ/kgK	c(T_i=195K) kJ/kgK	Theoretical kJ/kgK
Al	0.78±0.31	0.93±0.23	0.90
NaCl	1.66±3.11	1.64±2.71	0.85
C	0.56±0.15	0.66±0.11	0.71
Zn	0.39±0.13	0.50±0.11	0.39
Cu	0.35±0.10	0.41±0.09	0.38
Pb	0.14±0.04	0.17±0.02	0.13

An anomalous result was seen for the rock salt. The method for submerging this sample deviated from the standard method. This result should therefore be disregarded.

5 Discussion

5.1 Latent Heat of Vaporisation of N_2

The value obtained for the latent heat of vaporisation of 213.8±3.8 kJ/kg is greater than the theoretical value by 13.8 kJ/kg. The result is reliable yet inaccurate and the ease of the method allows for easily reproducible results.

The wire used in delivering heat to the system was the main source of error. A small part of the wire was resting in the nitrogen and the rest was outside of the system, subject to room temperatures. This allows the conduction of heat into the system through the wire. To correct this, surround the wire in a thermal jacket with only the heating element exposed and submerged in the nitrogen.

5.2 Heat Capacities using N_2

As shown by table 1, results are accurate and within the margin of error. Half of the results increase in accuracy when a lower initial temperature is used. Accuracy may further be improved if a more accurate result for the latent heat of vaporisation was obtained. However results are unreliable, due to the large difference in heat capacity values obtained from room temperature and dry ice.

Simple changes can eliminate human error and improve the accuracy of results. Measuring the temperature of samples before submersion would improve accuracy of results. It is important that samples have a high purity and are not subject to oxidation. It should be noted that the buoyancy force caused by introducing a sample into the nitrogen will result in convection currents within the nitrogen. This may cause an excess of boil off unaccounted for by the natural boil off result, where no convection current is present. Addressing this through further analysis at the natural boil off stage was needed. Using a mechanical device to lower samples in and out of the system will minimise this, reducing unnecessary kinetic energy production and human error.

A large change in mass at region C shown on figure 6, corresponds to a large store of energy and therefore heat capacity. The negative gradient of region C corresponds to thermal conductivity. A good example showing both of these features this would be graphite, where a large change in mass and negative gradient was observed.

The greatest change in mass at region C was seen by aluminium. This is due to aluminium having more atoms per gram than any other sample. More atoms corresponds to more degrees of freedom available to store energy, agreeing with theoretical predictions. Further evidence of this is seen throughout the samples. For example, an aluminium sample of 7.30g has 162.82×10^{21} atoms and a heat capacity of 0.90 kJ/kgK where. However a lead sample of 30.7g has 89.31×10^{21} atoms and a heat capacity of 0.13 kJ/kgK.

The largest negative gradient can be seen by graphite. Graphite has large spaced lattice structures allowing for the propagation of high energy phonons. With each phonon having a larger quantum of energy, it follows that its heat will dissipate quickly, agreeing with the results and theoretical predictions.

5.3 Heat Capacities using CO_2

The greater the change in temperature, the more violent the reaction. This corresponds to a greater approximation and therefore error in calculated heat capacities. An interpretation of this is shown by figure 7.

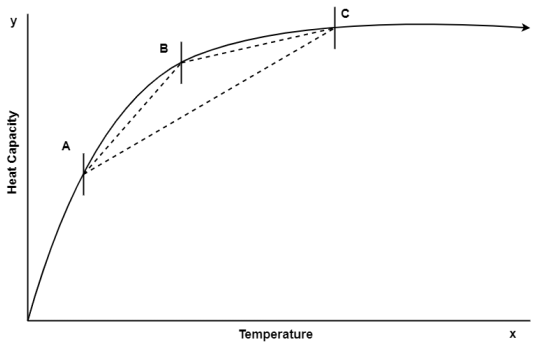

Figure 7: Interpretation of approximations made. A corresponds to 77K, B to 195K and C to 293K

The area enclosed by the dotted line shows the approximations made from different initial temperatures. Clearly the area enclosed from A to C is considerable in comparison with the area enclosed from A to B. This translates to more accurate results using smaller changes in temperature. Table 1 shows that only half of the results improve in accuracy by a small amount. This is likely due to the sample's initial temperature not reaching that of the dry ice. The sample is submerged in a beaker of dry ice but the entire surface area of the sample was not in direct contact.

The idea of reducing the initial temperature of the sample before submerging was of sound theory and reduces error in results, as shown by figure 7. Recording the initial temperature of the sample and not assuming it was that of the dry ice yields accurate initial temperature measurements and final results.

The experiment is well constructed providing a simple way of determining heat capacity of samples that agree well with theoretical values. The system is insulated well enough that boil off can be accounted for and therefore never affects results. Software and equipment used ensure that values obtained have small uncertainties. With relatively few changes accuracy can be improved. A better value for the latent heat of vaporisation of nitrogen could see the results improve greatly.

6 Conclusion

Samples of varying initial temperatures were placed into liquid nitrogen until a thermal equilibrium was reached. This causes a change in mass of the system which was recorded and used to calculate the heat capacity of samples.

Results of the experiment are consistently within margin of error for theoretical values, suggesting the method used was sound. Accuracy and reliability can be greatly improved with minor changes and further system analysis previously stated.

It was concluded that samples containing a higher number of atoms per gram have higher heat capacities, due to greater numbers of degrees of freedom. Furthermore, evidence suggests that a larger lattice structure corresponds to higher thermal conductivity, although further research is needed.

Important future improvements include using an insulated jacket around the wire used to supply heat to the system. Measuring the temperature of each sample before submersion to acquire accurate initial temperatures. Using mechanical lowering device to insert samples into the system. Analysis of convection currents upon sample entry into system. Such changes could see a highly accurate heat capacity measurement.

7 Appendix

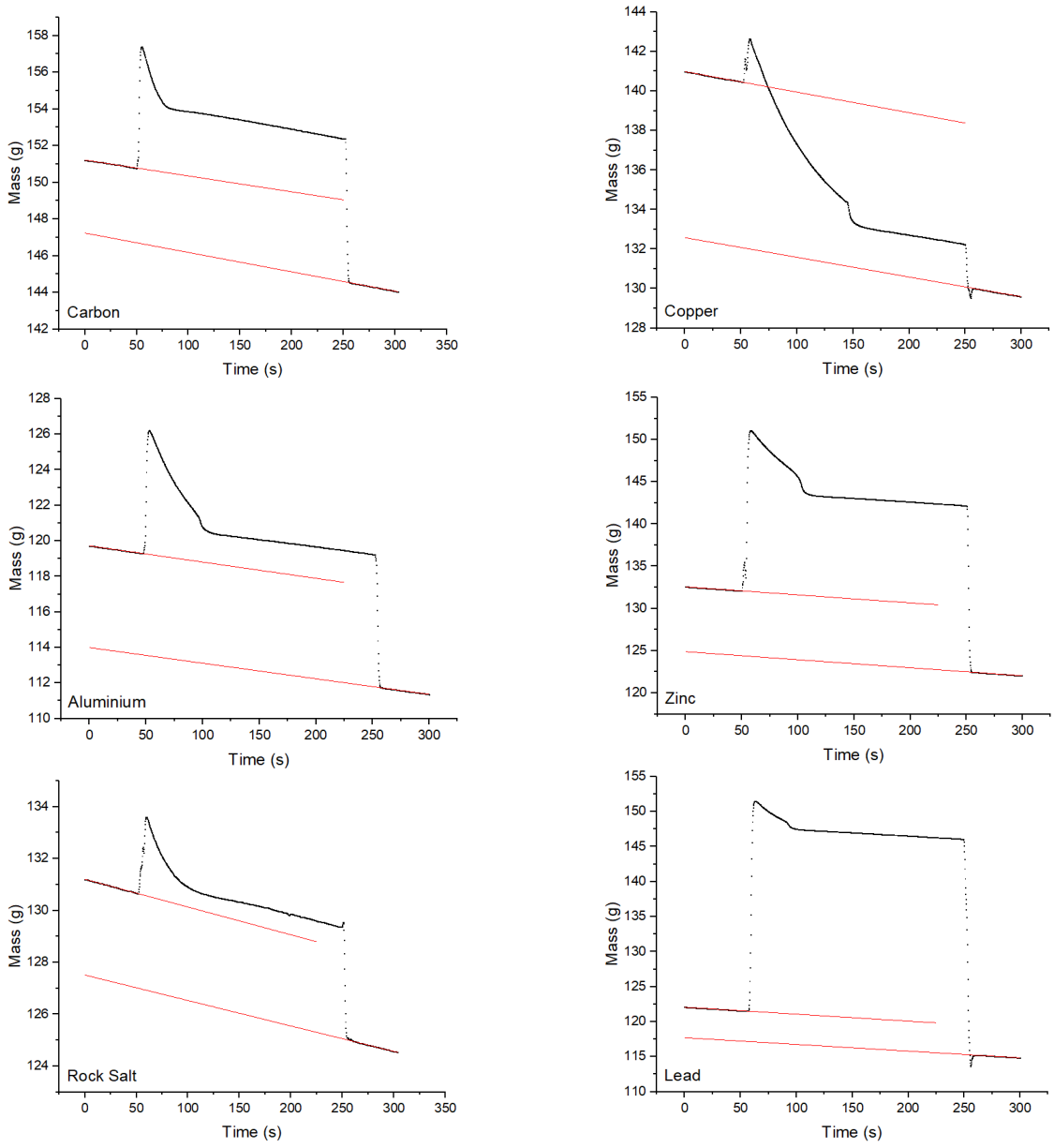

Figure 8: Change in mass of system overtime using liquid nitrogen for samples, a) Carbon, b) Copper, c) Aluminium, d) Zinc, e) Rock salt, f) Lead.

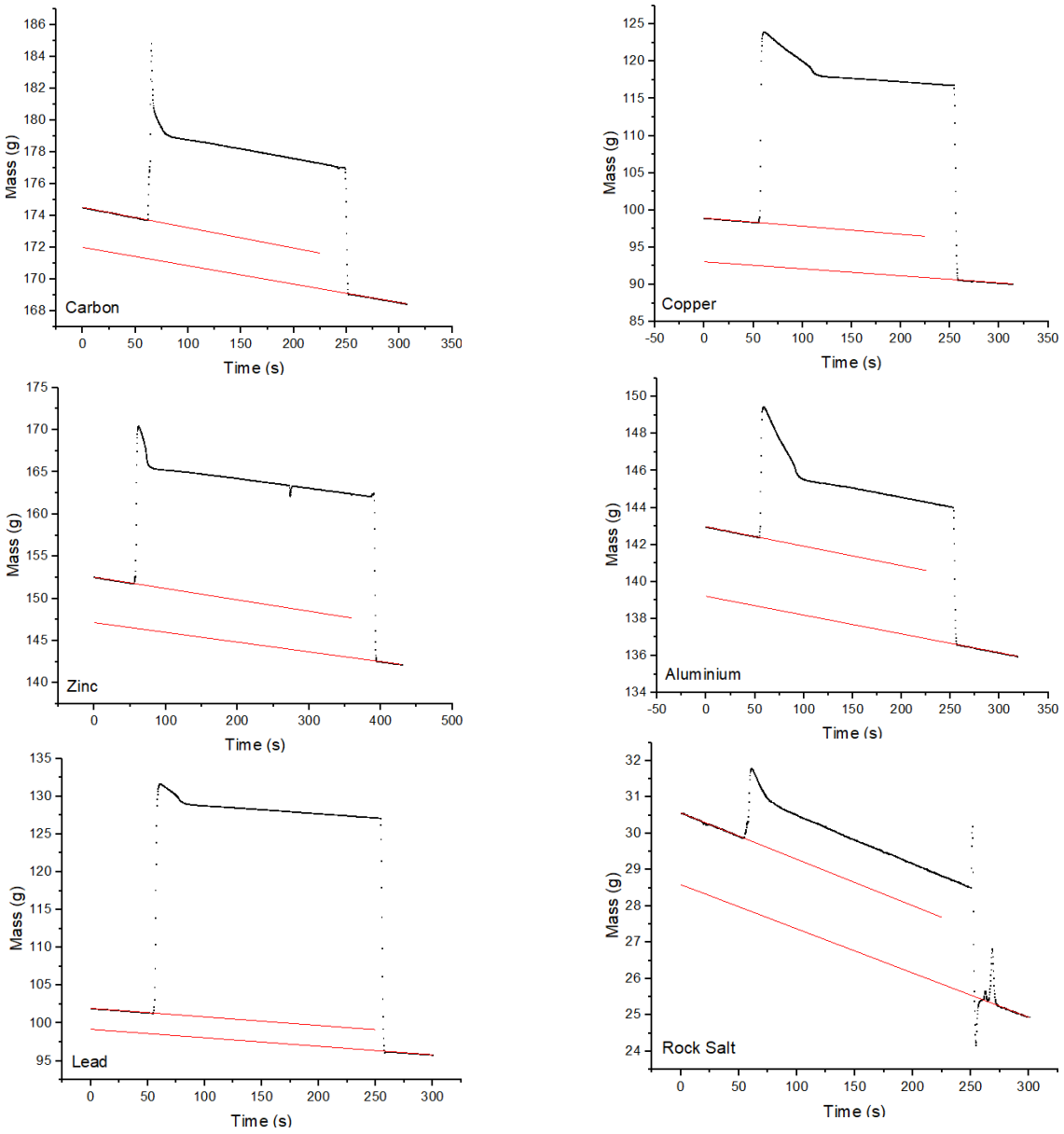

Figure 9: Change in mass of system overtime using dry ice for samples, a) Carbon, b) Copper, c) Zinc, d) Aluminium, e) Lead, f) Rock salt.

References

[1] Douglas L Martin. The specific heat of copper from 20 to 300 deg; k. *Canadian Journal of Physics*, 38(1):17–24, 1960.

[2] Theodore William Richards and Arthur Becket Lamb. New methods of determining the specific heat and the reaction-heat of liquids. In *Proceedings of the American Academy of Arts and Sciences*, volume 40, pages 659–680. JSTOR, 1905.

[3] Donghyun Shin and Debjyoti Banerjee. Enhancement of specific heat capacity of high-temperature silica-nanofluids synthesized in alkali chloride salt eutectics for solar thermal-energy storage applications. *International journal of heat and mass transfer*, 54(5-6):1064–1070, 2011.

[4] RA Fisher, JE Gordon, and NE Phillips. Specific heat of the high-t c oxide superconductors. *Journal of Superconductivity*, 1(3):231–294, 1988.

[5] Prem Datt. *Latent Heat of Vaporization/Condensation*, pages 703–703. Springer Netherlands, Dordrecht, 2011.

[6] Douglas W Waples and Jacob S Waples. A review and evaluation of specific heat capacities of rocks, minerals, and subsurface fluids. part 1: Minerals and nonporous rocks. *Natural resources research*, 13(2):97–122, 2004.

[7] David G Cahill and Robert O Pohl. Lattice vibrations and heat transport in crystals and glasses. *Annual review of physical chemistry*, 39(1):93–121, 1988.

[8] Raphaël P Hermann, Fernande Grandjean, and Gary J Long. Einstein oscillators that impede thermal transport. *American journal of physics*, 73(2):110–118, 2005.

[9] AJ Dekker. Solid state, 1962.

[10] Charles Kittel. Introduction to solid state physics. *American Journal of Physics*, 35(6):547–548, 1967.

[11] Jacob Bernard John Chapman. *Improving the Functional Control of Ferroelectrics Using Insights from Atomistic Modelling*. PhD thesis, UCL (University College London), 2018.

[12] Walter A Harrison. *Electronic structure and the properties of solids: the physics of the chemical bond*. Courier Corporation, 2012.